

Article

A Study on the Aging Behavior of Nitrided W18Cr4V Steel in High-Temperature Sodium

Xiaogang Fu ¹, Na Liang ¹, Wei Zhang ¹, Liu Tao ¹, Bo Qin ¹, Zhangshun Ruan ¹ , Bin Long ^{1,*} and Shasha Lv ^{2,*}

¹ Reactor Engineering Technology Research Department, China Institute of Atomic Energy, Xinzhen, Fangshan District, Beijing 102413, China; fuxiaogang09@126.com (X.F.); 15801268865@163.com (N.L.); 02041119@163.com (W.Z.); tao2013liu@163.com (L.T.); 13811250420@139.com (B.Q.)

² Key Laboratory of Beam Technology, Ministry of Education, College of Nuclear Science and Technology, Beijing Normal University, Beijing 100875, China

* Correspondence: bin.long@hotmail.com (B.L.); lvss@bnu.edu.cn (S.L.)

Abstract: The loading and unloading elevators are the primary equipment in the refueling system, used for transferring fuel assemblies in the sodium-cooled fast reactors. The guideway friction pairs are the critical components of these elevators in the refueling system. With the excellent hardness and wear resistance in air, nitrided W18Cr4V steel is a promising material for the guideway friction pairs. In order to assess the feasibility of using nitrided W18Cr4V steel, it is essential to understand the aging behavior of nitrided W18Cr4V steel in high-temperature sodium. Aging tests were conducted on nitrided W18Cr4V steel in sodium and in argon environments at various temperatures for different exposure times. The results showed that the nitrogen atoms in the nitrided layer exhibited bidirectional diffusion behavior in the sodium or argon environment at 540 °C. Compared to the argon environment, cracks formed within the nitrided layer and the diffusion of nitrogen into the sodium was accelerated in the nitrided layer. As a significant number of nitrogen atoms had diffused into the sodium, there was little difference in the hardness between nitrided W18Cr4V steel and non-nitrided W18Cr4V steel after long-term exposure to 540 °C sodium.

Keywords: fast reactor; nitrided W18Cr4V steel; high-temperature sodium; aging behavior



Citation: Fu, X.; Liang, N.; Zhang, W.; Tao, L.; Qin, B.; Ruan, Z.; Long, B.; Lv, S. A Study on the Aging Behavior of Nitrided W18Cr4V Steel in High-Temperature Sodium. *Metals* **2024**, *14*, 357. <https://doi.org/10.3390/met14030357>

Academic Editors: Facundo Almeraya-Calderón, José Guadalupe Chacón-Nava, Enrique Vera-López and Citlalli Gaona-Tiburcio

Received: 13 February 2024

Revised: 10 March 2024

Accepted: 16 March 2024

Published: 19 March 2024



Copyright: © 2024 by the authors. Licensee MDPI, Basel, Switzerland. This article is an open access article distributed under the terms and conditions of the Creative Commons Attribution (CC BY) license (<https://creativecommons.org/licenses/by/4.0/>).

1. Introduction

The liquid-cooled fast reactors have the primary function of transmuting long-lived and high-level radioactive fission products into short-lived or non-radioactive nuclides using fast neutrons. Furthermore, the liquid-cooled fast reactors have remarkable safety characteristics, resulting to a large extent from the fact that the reactor is a low-pressure system with large thermal inertia and a negative temperature coefficient. Therefore, the long-term development of nuclear energy requires liquid-cooled fast reactor technology. Throughout the fast reactor history, the sodium coolant has been the highly efficient heat carrier that is applied most commonly. The sodium-cooled fast reactor is the closest to commercialization for nuclear plants amongst the six types of fourth-generation reactors, as announced at the Generation IV International Forum [1–7]. The high-temperature sodium in the reactor vessel is covered with argon to prevent strong chemical activity. The concentration of the fissile isotope nuclides is decreasing during fast reactor operation. Excess fissile material above the critical mass is loaded into the core and the excess reactivity is compensated for by the control rods. The loading of new fuel assemblies ensures nominal operation until the next refueling. Then, some spent fuel assemblies would be unloaded from the core, and new fuel assemblies would be loaded in the core. The refueling system has been specifically designed for fuel assembly loading and unloading in a sodium-cooled fast reactor [8–10].

The refueling system of the sodium-cooled fast reactor comprises an in-reactor refueling system, out-of-reactor refueling system, new fuel assembly transfer system, and

spent fuel assembly transfer system. The normal operation of these systems relies on the coordinated work of various primary equipment in the reactor vessel. The primary equipment comprises the core, the large plug, the small plug, the fuel handling machine, the fuel loading elevator, the fuel unloading elevator, etc. [11,12]. In the refueling process of the sodium-cooled fast reactor, the fuel loading elevator and the fuel unloading elevator play an important role. They are responsible for transporting a new fuel assembly from the outside of the reactor to the inside, and transporting the spent fuel assembly from the inside to the outside. The guide rail friction pair is a crucial component of the fuel loading elevator and the fuel unloading elevator, consisting of a guide rail and a slider, used to support and guide the transportation of the fuel assembly. Throughout the period of reactor operation, the guide rail is continuously exposed to a high-temperature-sodium environment, while the slider performs a reciprocating motion during the refueling process for the transportation of the fuel assembly. The operational conditions of the guide rail friction pair require the manufacturing material to have excellent high-temperature sodium compatibility, high hardness, and high wear resistance. The W18Cr4V steel has been used to manufacture the guide rail friction pairs of the sodium-cooled fast reactor elevators. In order to extend the service life, it is necessary to improve the surface hardness and wear resistance of W18Cr4V steel. Compared to W18Cr4V steel, nitrided W18Cr4V steel exhibits higher hardness, wear resistance, and heat resistance. Furthermore, nitrogen exhibits low solubility in high-temperature-sodium environments, which means that nitrided W18Cr4V steel may have high chemical stability in high-temperature sodium and is anticipated to exhibit favorable compatibility with sodium at high temperatures. Therefore, nitrided W18Cr4V steel might be an ideal candidate material for manufacturing guide rail friction pairs for sodium-cooled fast reactor elevators, with the potential to meet the requirements of guide rail friction pairs in high-temperature-sodium environments [13–15].

Nitriding treatment is a surface modification technology widely used in the industrial field. Through the nitriding process, a uniform and hard nitrided layer can be formed on the surface of the material, which can significantly improve the surface hardness and wear resistance of the material, thereby extending the service life of the components. In many industrial applications, the nitriding processes have proven their effectiveness in improving component performance [16–21]. Nevertheless, while nitrided steels demonstrate excellent performance in air environments, there are relatively few studies regarding their behavior and performance evaluation in sodium at high temperatures [22–26]. Therefore, it is essential to investigate the aging characteristics of nitrided W18Cr4V steel in high-temperature-sodium environments to ensure the reliable operation of guide rail friction pairs. At the same time, in order to determine the feasibility of using nitrided W18Cr4V steel for the manufacturing of guide rail friction pairs, a series of aging tests at different temperatures and durations are needed. The purpose of these tests is to understand the aging behavior of the nitrided layer in a high-temperature-sodium environment, investigate the diffusion mechanism of nitrogen atoms, accurately understand the hardness changes in nitrided W18Cr4V steel after long-term aging in high-temperature sodium, and evaluate whether it could meet the requirements of guide rail friction pairs. In addition, these research results will provide an important basis for the design and material selection of guide rail friction pairs in sodium-cooled fast reactors, and help to improve the operational reliability of fuel loading elevators and fuel unloading elevators.

2. Methods

2.1. Materials

The range of chemical compositions of W18Cr4V steel are shown in Table 1. According to the experimental requirements, the original samples were cut into sheet samples of size 8.8 mm × 8.8 mm × 2 mm. To meet the experimental requirements for sample surface roughness, the cut sheet samples were ground in turn with sandpapers of 200#, 400#, 800#, 1200#, 1500#, 2000#, and 3000#. The surface of W18Cr4V steel is treated with ion nitriding in order to form a nitrided layer.

Table 1. The range of chemical compositions of W18Cr4V steel.

| Elements | C | Mn | Si | Mo | Cr | W | V | Fe |
|----------|---------|------|------|------|---------|-----------|---------|-----|
| wt.% | 0.7–0.8 | ≤0.4 | ≤0.4 | ≤0.3 | 3.8–4.4 | 17.5–19.0 | 1.0–1.4 | Bal |

Prior to ion nitriding, the W18Cr4V steel samples were cleaned by argon ion bombardment to remove the oxide layers that had formed on the surface. Subsequently, the samples were ion nitrided using a mixture of nitrogen and hydrogen gas at 520 °C for 1 h. After completing the ion nitriding process, the samples were slowly cooled in the chamber to room temperature. The technical criterion for the samples is specified as follows: the nitrided layer should have a minimum thickness of 40 μm, and its initial microhardness should exceed 1000 HV_{0.1}. Secondly, the sample's surface should be free of any oxide layer.

The microstructure of W18Cr4V steel before nitriding treatment is illustrated in Figure 1a. It can be seen that there are many white particles in the material matrix, which are tungsten compounds that can improve the hardness and wear resistance at high temperatures. The X-ray diffraction (XRD) result of W18Cr4V steel before and after the ion nitriding process is shown in Figure 1b. The XRD pattern of nitrided W18Cr4V steel reveals diffraction peaks corresponding to ε-Fe₃N, α-Fe, and Fe₃W₃C. ε-Fe₃N is an iron nitride, which signifies the existence of the nitrided layer. The α-Fe phase is an oversaturated solid solution and it contains a specific quantity of nitrogen atoms, which occupy interstitial positions within the α-Fe lattices. The α-Fe phase is the earliest phase during the process of nitriding. Fe₃W₃C is a carbide that contains the elements of tungsten and iron, and it is the primary carbide in W18Cr4V steel [27–30]. In comparison to the non-nitrided W18Cr4V steel, the XRD pattern of the nitrided W18Cr4V steel shows diffraction peaks of ε-Fe₃N. Additionally, the diffraction peaks of α-Fe (110) and (200) have shifted to the left.

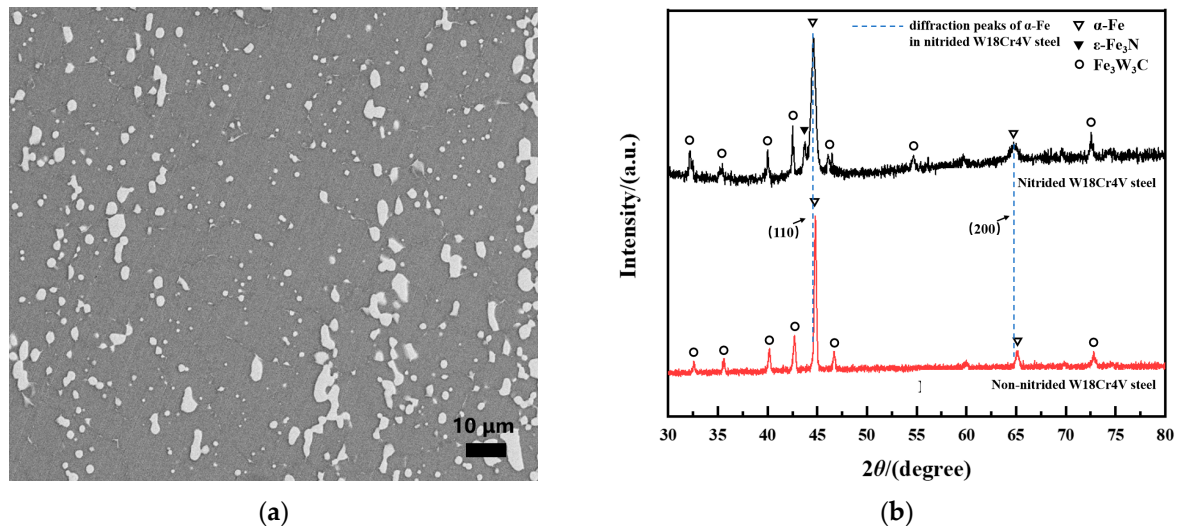


Figure 1. The characterization results of W18Cr4V steel before and after the ion nitriding process: (a) The microstructure of W18Cr4V steel before ion nitriding process, (b) The XRD result of W18Cr4V steel before and after ion nitriding process.

2.2. Experiment

In order to analyze the different aging behaviors of nitrided W18Cr4V steel in sodium and argon at high temperature, nitrided W18Cr4V steel had been subjected to the comparative aging tests in a sodium or argon environment at 540 °C for 200 h and 500 h. All the sheet samples were capsuled into different claddings of 304 stainless steel. The diameter of claddings was 28 mm and the length was 70 mm. For the high-temperature sodium behavior tests, the claddings were filled with the sodium that the samples were immersed in and the cladding gap was filled with high-purity argon gas. For the high-temperature-argon

behavior tests, the claddings were fully filled with argon and the samples were immersed in the high purity argon environment. The comparative aging tests were carried out in the tube furnaces under an argon gas environment. The uncertainty of temperature in the tube furnace was ± 3 °C.

After the comparative aging tests, the claddings were cut along the upper part of tube. The claddings containing the sodium and samples were placed on a heating plate at 150 °C. So, the sodium was melted and the samples were removed from the claddings. The samples with residual sodium on the surface were cleaned in alcohol at room temperature. As the remaining sodium reacted with the alcohol, bubbles were formed on the surface of the samples and moved to the surface of the alcohol. When the bubbles were no longer generated, it meant that the residual sodium had been removed completely. The cleaning time in alcohol was approximately 1 h to 1.5 h due to the difference in the residual sodium quality. The samples that contained the argon gas only were removed directly from the claddings after cutting. All the samples had been washed twice in high-purity water for 5 min each by an ultrasonic cleaning machine. Finally, all the samples were dried with cold air to remove the water on the surface and placed in the drying cabinet at 60 °C for one hour. Part of the samples were cut into two pieces and the cross sections were prepared by mechanical grinding and polishing. The hardness on the cross section of samples was measured with a MicroMet 5104 Hardness Tester using a load of 100 g, which was produced by the BUEHLER Company in Lakecraft, IL, USA. The maximum error in the hardness measurement was less than 6%. Samples before and after the comparative aging tests were characterized by a symmetrical geometric X-ray diffraction analysis. XRD measurements were performed utilizing a D8 Advance X-ray diffractometer manufactured by the Bruker Company in Germany, with a Cu-K α ($\lambda = 1.5418$ Å) source. Samples were further examined using a field emission scanning electron microscope (SEM). The SEM model utilized was the Supra55, produced by the Zeiss company in Jena, Germany.

In order to observe the long-term aging behavior of nitrided W18Cr4V steel in high-temperature sodium, the accelerated aging tests of nitrided W18Cr4V steel and W18Cr4V steel were carried out in 700 °C sodium for 2 h, 3.6 h, 143.4 h, 255.9 h, and 308.3 h. The sample size of nitrided W18Cr4V steel and W18Cr4V steel is 8.8 mm \times 8.8 mm \times 2 mm. The samples were also capsuled into the same claddings of 304 stainless steel mentioned above. The procedures for the accelerated aging test and sample cleaning were the same as those described above. After the tests, the cross section of the samples was ground and polished and the microhardness at the cross section of the samples was measured by a microhardness tester.

3. Results and Discussions

3.1. Aging Behavior of Nitrided W18Cr4V Steel in High-Temperature Sodium and Argon

When the nitrided W18Cr4V steel is subjected to the aging test in the sodium and argon at a high temperature for a duration of time, an obvious variation in the nitride layer would be generated. The thickness of the nitrided layer would be increasing while the microhardness would be decreasing significantly.

Figure 2 illustrates the microhardness profiles of W18Cr4V steel subjected to ion nitriding and subsequent aging tests in sodium and argon environments at 540 °C for 200 h. The initial nitride layer thickness in the W18Cr4V steel is approximately 60 μ m, determined by microhardness variation at the cross section. The microhardness of the nitrided layer ranges between 1127.8 Hv_{0.1} and 1110.1 Hv_{0.1}, while the microhardness of the steel matrix ranges from 882.5 Hv_{0.1} to 858.3 Hv_{0.1}. It suggests the formation of a hardness gradient on the steel surface due to the ion nitriding process, with the microhardness in the nitrided layer being directly proportional to the nitrogen content. Exposure to argon aging for 200 h at 540 °C resulted in an expansion of the nitrided layer thickness to about 160 μ m, accompanied by the decrease in microhardness with the values in the range from 802.1 Hv_{0.1} to 741.5 Hv_{0.1}. It indicates that the nitrogen atom diffusion processes in a high-temperature-argon environment had influences on the thickness and the hardness of

the nitrided layer. Meanwhile, the high temperature also caused a decrease in the hardness of the W18Cr4V steel matrix, as the matrix's microhardness also decreased with the valves ranging from 741.5 $Hv_{0.1}$ to 650.9 $Hv_{0.1}$. Conversely, exposure to sodium aging for 200 h at 540 °C led to an increase in the nitrided layer's thickness to approximately 93 μm . The microhardness values exhibited a more significant decrease, ranging from 746.3 $Hv_{0.1}$ to 530.1 $Hv_{0.1}$, while the matrix's microhardness decreased with the valves varying between 658.9 $Hv_{0.1}$ and 624.4 $Hv_{0.1}$. This suggests that sodium exposure induces different nitrogen atom diffusion behavior, altering the characteristics of the nitrided layer. The result above indicates nitrogen atoms within the nitrided layer can not only diffuse into the sodium or argon environments outward but also can migrate into the W18Cr4V steel matrix inward. This bidirectional diffusion behavior of nitrogen atoms demonstrates the reasons for the variations in the nitrided layer, and it is sensitive to the environmental factors. Despite the low solubility of nitrogen in high-temperature sodium, the concentration of nitrogen atoms within the nitrided layer reaches a supersaturated state. This saturation serves as the driving force for the bidirectional diffusion of nitrogen atoms. The high concentration of nitrogen atoms within the layer influences both the outward diffusion into the environment and the inward diffusion into the material matrix.

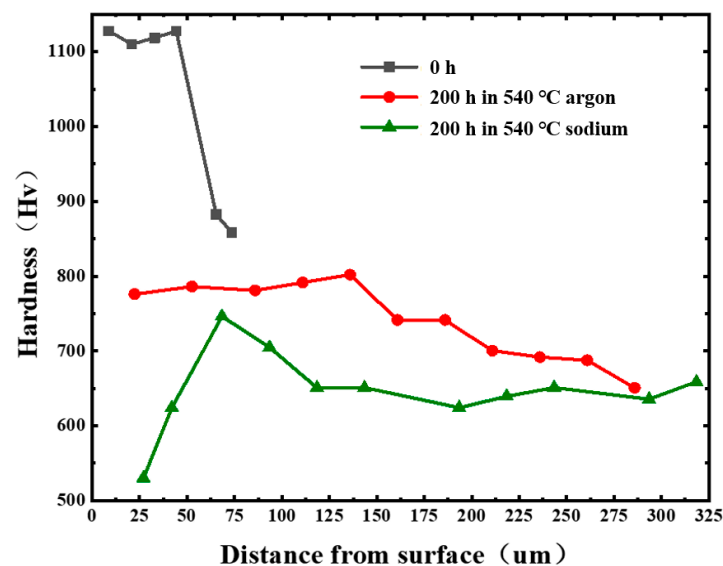


Figure 2. The microhardness test results of nitrided W18Cr4V steel after 200 h aging in sodium and argon at 540 °C.

Figure 3 presents the results of microhardness tests conducted on nitrided W18Cr4V steel after the aging test in sodium and argon environments at high temperature for different durations. Figure 3a illustrates the results of microhardness testing after the aging experiments in a sodium environment at 540 °C. Following 200 and 500 h of aging, the thickness of the nitrided layer had increased to 93 μm and 130 μm , respectively. However, it is noteworthy that in the region 30 μm from the sample surface, the microhardness values significantly decreased to 530.1 $Hv_{0.1}$ and 479.5 $Hv_{0.1}$, respectively. The maximum hardness values within the nitrided layer reached 746.3 $Hv_{0.1}$ and 718.4 $Hv_{0.1}$ respectively, and the positions of these maximum values shifted inward by approximately 10 μm relative to the material matrix. In contrast, the results of the aging test in an argon atmosphere at 540 °C are depicted in Figure 3b. Under this condition, the thickness of the nitrided layer increased significantly, reaching 185 μm after 200 h and 232 μm after 500 h. The microhardness values near the 30 μm depth decreased to 776 $Hv_{0.1}$ and 631.9 $Hv_{0.1}$ respectively. The maximum hardness values within the nitrided layer were 802.1 $Hv_{0.1}$ and 736.8 $Hv_{0.1}$, respectively, and these maximum values shifted inward by approximately 46 μm relative to the material matrix.

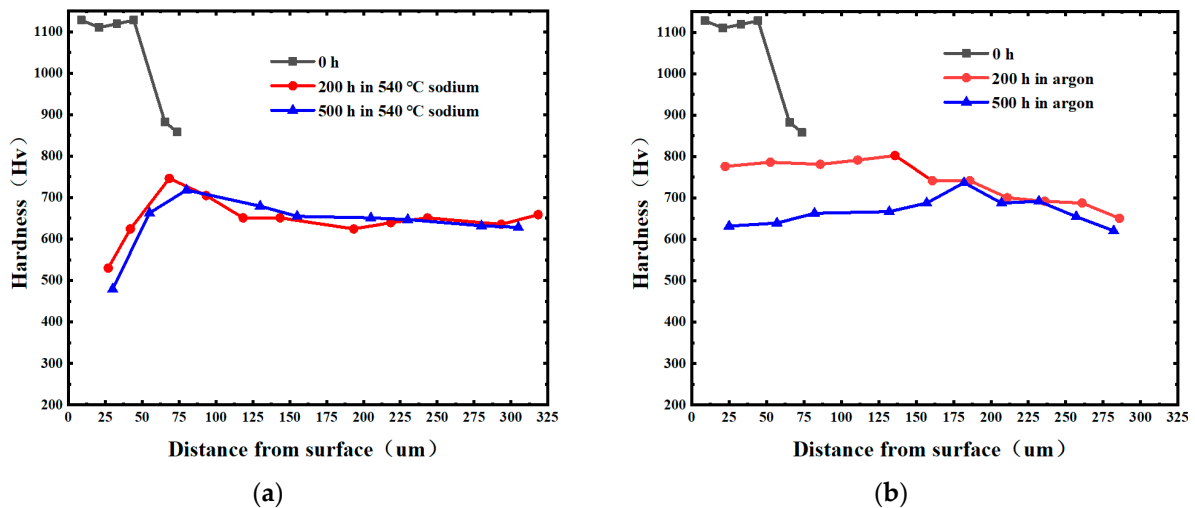


Figure 3. The results of the microhardness examinations of nitrided W18Cr4V steel before and after aging tests: (a) aging in sodium at 540 °C for 200 h and 500 h, (b) aging in argon at 540 °C for 200 h and 500 h.

The growth of the nitrided layer's thickness when aged in a sodium environment is notably less than that in an argon environment. The reduction in microhardness at a depth of approximately 30 μm within the nitrided layer of W18Cr4V steel, when subjected to aging in a sodium environment, is notably more pronounced compared to aging in an argon environment. It suggests that the presence of sodium has a more pronounced influence on the hardness of the nitrided layer. The rate of nitrogen atom diffusion from the nitrided layer into sodium is greater than that into argon. Figure 4 illustrates the SEM observation results of the aging test of nitrided W18Cr4V steel after 200 h in sodium and argon at 540 °C, respectively. From Figure 4a, it is evident that following exposure to a sodium environment, numerous cracks developed within the nitrided layer. Nevertheless, from Figure 4b, it is observed that after aging in an argon environment, no cracks were found in the nitrided layer. In sodium at 540 °C, the nitrogen and other alloy elements in the nitrided layer diffuse and dissolve into the sodium, meanwhile a number of crystal defects are formed within the nitrided layer. These crystal defects increase the diffusion rate of elements, leading to accelerated dissolution into the sodium, and ultimately, forming cracks at various positions within the nitrided layer. The presence of cracks enhances the contact area between the nitrided layer and high-temperature sodium, further promoting the dissolution of nitrogen and other alloy elements into the sodium. Therefore, in sodium at 540 °C, the diffusion and dissolution of nitrogen and other alloy elements in the nitrided layer into the sodium are significantly accelerated, which continuously results in crack formation. In argon at 540 °C, only nitrogen diffuses into the argon from the nitrided layer, with few other alloy elements lost to the argon. Therefore, cracks do not form in the nitrided layer, and the diffusion rate of nitrogen atoms into the argon does not increase. In summary, in a sodium environment at 540 °C, the outward diffusion rate of nitrogen atoms is significantly higher than in an argon environment, which also results in crack formation in the nitrided layer. Owing to the accelerated rate of nitrogen atom depletion in a sodium environment, the concentration of nitrogen atoms on the surface of the sample is decreased, leading to a greater concentration gradient and faster diffusion of nitrogen atoms to the surface. Consequently, this results in a lesser increase in the thickness of the nitrided layer. Upon aging in sodium, the maximum microhardness value in the nitrided layer is observed to be lower compared to aging in argon. Additionally, the distance of the maximum microhardness value moving towards the material matrix is also found to be smaller in sodium.

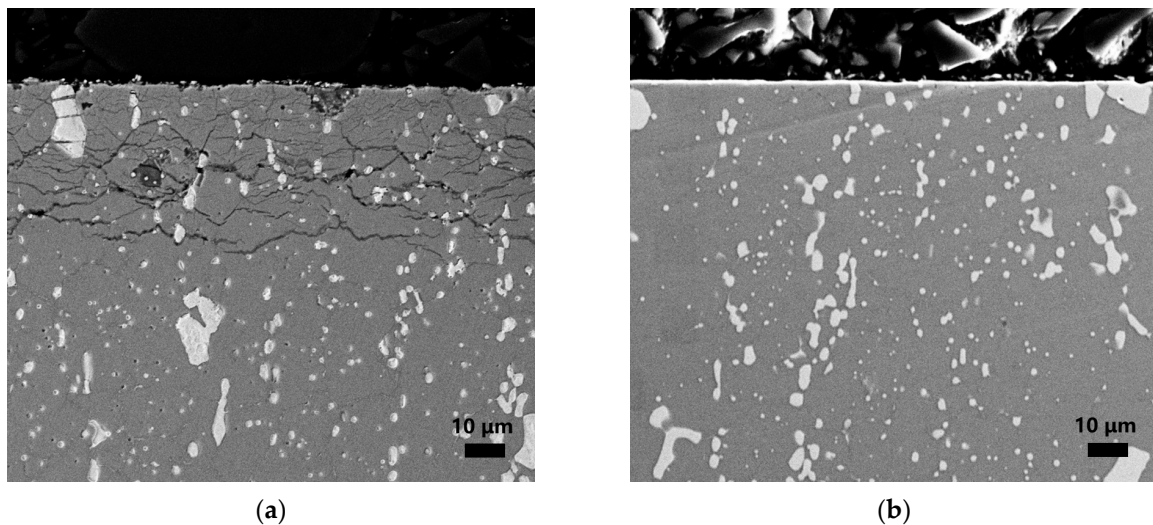


Figure 4. The SEM results of nitrided W18Cr4V steel after 200 h aging in sodium and argon at 540 °C: (a) aging in sodium, (b) aging in argon.

Figure 5 illustrates the XRD results of nitrided W18Cr4V steel before and after being subjected to sodium and argon environments at 540 °C for 200 h and 500 h, respectively. After aging tests in sodium and argon environments at 540 °C, the diffraction peak of ϵ -Fe₃N vanishes, while the position of the diffraction peak of α -Fe noticeably shifts to the right. The vanish of the diffraction peak of ϵ -Fe₃N suggests a decrease in the nitrogen content within the nitrided layer. The nitrogen atoms exhibit a bidirectional diffusion behavior, leading to a decrease in nitrogen content at the surface and an increase in the thickness of the nitrided layer. For the non-aging nitrided W18Cr4V steel, nitrogen atoms occupy interstitial positions within the α -Fe lattices. Once the concentration of nitrogen atoms surpasses a specific threshold, there is a notable expansion of the iron atom lattice, leading to an increase in the crystallographic parameters and a decrease in the 2θ angle of the corresponding diffraction peak [31]. In comparison to the non-nitrided W18Cr4V steel, the diffraction peak positions of α -Fe (110) and (200) in the nitrided layer are observed to shift to the left. Following aging tests in a sodium and argon environment at 540 °C, the nitrogen content in the nitrided layer significantly decreases due to bidirectional diffusion of nitrogen atoms. This results in a decrease in the iron lattice expansion and a reduction in the crystallographic parameters. Consequently, the diffraction peak of α -Fe (110) and (200) shifts to the right noticeably. The absence of the diffraction peak of ϵ -Fe₃N and the displacement to the right of the diffraction peak of α -Fe suggest that the bidirectional diffusion of nitrogen atoms results in a reduction in nitrogen content within the nitrided layer and a decrease in microhardness values in the same layer. The loss of nitrogen atoms in the nitrided W18Cr4V steel is more pronounced in a sodium environment, leading to a more significant reduction in the strengthening effect caused by the nitriding process.

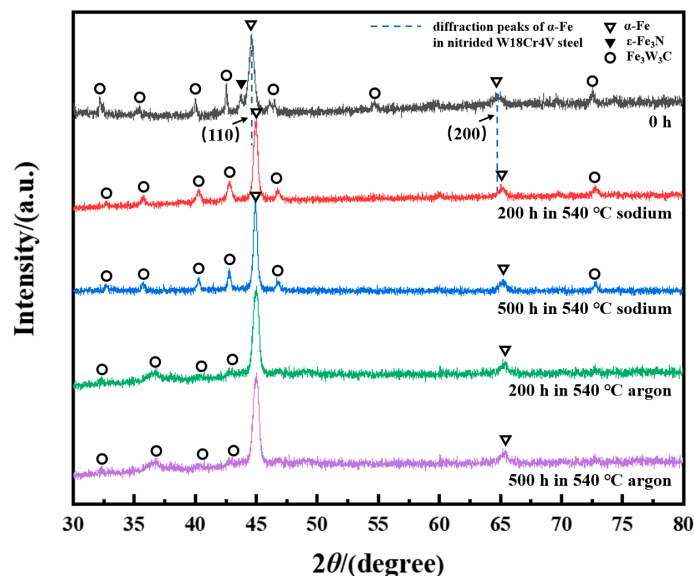


Figure 5. The XRD patterns of nitrided W18Cr4V steel before and after aging in sodium and argon environments at 540 °C for 200 h and 500 h.

3.2. Accelerated Aging Behavior of Nitrided W18Cr4V Steel in High-Temperature Sodium

In a sodium environment at 540 °C, the surface microhardness of nitrided W18Cr4V steel was gradually decreasing with time, indicating that the strengthening effect of the nitriding process may not be able to be maintained for long. In order to confirm the long-term sustainability of the high hardness exhibited by nitrided W18Cr4V steel, it is essential to compare the trend in microhardness reduction in nitrided W18Cr4V steel with non-nitrided W18Cr4V steel at elevated temperatures in a sodium environment. This comparison would also enable the evaluation of the long-term stability of the structure and the performance of the nitrided layer. The Larson–Miller parameter method based on the Arrhenius equation was used in the accelerated aging test for accelerated aging behavior evaluation, as it could simulate the aging phenomenon of the materials in long-term service. This is achieved by elevating the test temperature of sodium, which can effectively compress several decades of service life into a shorter period, in order to assess the aging characteristics of materials. Through the accelerated aging tests in sodium with the temperature above 540 C, the data and the patterns of microhardness changes for the nitrided layer of W18Cr4V steel can be obtained for evaluating the long-term stability. If the microhardness of the nitrided W18Cr4V steel decreases slowly, it indicates good stability of the nitrided layer, which can maintain high hardness for a longer period of time. Conversely, if the microhardness decreases rapidly, it indicates poor stability of the nitrided layer, and the strengthening effect may not be maintained for a long time.

In this study, the microhardness test results were selected as the performance evaluation index for the comparison of the trends in performance changes between nitrided W18Cr4V steel and non-nitrided W18Cr4V steel after accelerated aging tests in a high-temperature-sodium environment. The Larson–Miller parameter equation used for the accelerated aging tests of the samples above in a sodium environment at 700 °C is as follows [32]:

$$LMP = T [12 + \lg(t)] \quad (1)$$

In this equation, *LMP* represents a specific performance value of the material. In this study, the microhardness test results were selected as the specific performance values. “*T*” represents the experimental temperature in Kelvin; “*t*” represents the experimental time in hours; “12” is a parameter of the material, determined based on the microhardness values obtained from aging tests of W18Cr4V steel at various temperatures and times. The Larson–Miller parameter method allows for the conversion of experimental time in a

sodium environment at 700 °C into the service time in an equivalent sodium environment at 540 °C. Under the conditions of an experimental temperature of 700 °C, the experimental times in the sodium environment for nitrided W18Cr4V steel and non-nitrided W18Cr4V steel were 2 h, 3.6 h, 143.4 h, 255.9 h, and 308.3 h, respectively. By using the Larson–Miller parameter method, the experimental times above correspond to 0.06 years, 0.12 years, 10 years, 20 years, and 25 years in an equivalent sodium environment at 540 °C, respectively, Figure 4 shows the results of accelerated aging tests of the nitrided W18Cr4V steel and non-nitrided W18Cr4V steel in a sodium environment at a temperature of 700 °C.

Figure 6 illustrates the microhardness changes in nitrided W18Cr4V steel and non-nitrided W18Cr4V steel after accelerated aging tests in sodium at 700 °C. As is shown in the figure, the microhardness of both materials had decreased sharply in the initial stage and then the decrease rate would gradually slow down. In the subsequent test period after the initial stage, the hardnesses of nitrided W18Cr4V steel and non-nitrided W18Cr4V steel remained in the range of 253Hv_{0.1} and 430Hv_{0.1} at a distance of 30 µm from the sample surface. This result indicates that although nitriding treatment can significantly improve the initial hardness of W18Cr4V steel, the high-temperature-sodium environment would promote the diffusion rate of nitrogen atoms, leading to a significant decrease in the nitrogen content in the nitrided layer. The loss would not only lead to a decrease in the nitrogen content within the nitrided layer but also result in a gradual diminishment of the strengthening effect induced by the nitriding process. The difference in microhardness between nitrided W18Cr4V steel and non-nitrided W18Cr4V steel become smaller after long-term service with the loss of nitrogen atoms. In some cases, the microhardness of nitrided W18Cr4V steel was lower than that of non-nitrided W18Cr4V steel. Compared with non-nitrided W18Cr4V steel, for the long service time in sodium at 540 °C, nitrided W18Cr4V steel no longer has the significant performance advantages.

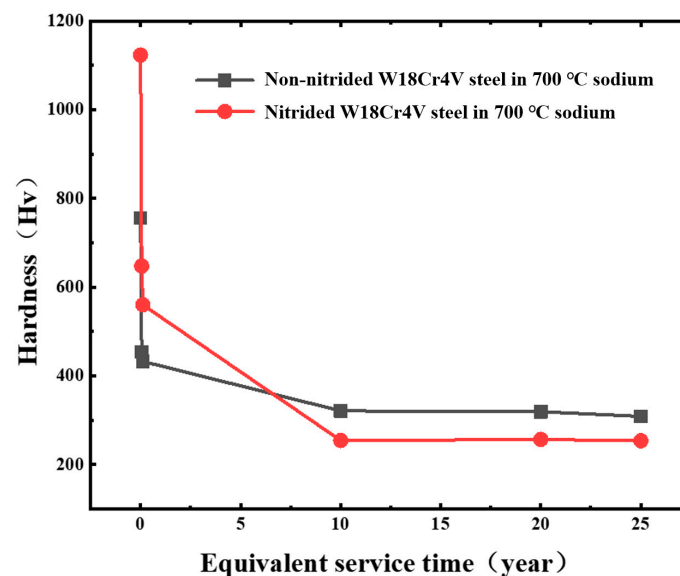


Figure 6. The results of accelerated tests conducted on nitrided W18Cr4V steel and non-nitrided W18Cr4V steel in a sodium environment at a temperature of 700 °C.

4. Conclusions

In order to understand the aging behavior of nitrided W18Cr4V steel in high-temperature sodium, comparative aging tests were conducted on nitrided W18Cr4V steel in sodium and in argon at the temperature of 540 °C. At the same time, accelerated aging tests using the Larson–Miller parameter method were performed on nitrided W18Cr4V steel in a sodium environment at the temperature of 700 °C. Based on the above test results, the following conclusions were drawn:

Firstly, the nitrogen atoms in the nitrided layer of W18Cr4V steel exhibit bidirectional diffusion behavior in a sodium or argon environment at 540 °C. This indicates that nitrogen atoms not only diffuse into the sodium or argon environment, but also penetrate into the interior of the W18Cr4V steel matrix. This bidirectional diffusion leads to a decrease in the microhardness of the nitrided layer, an expansion in the thickness of the nitrided layer, the absence of the ϵ -Fe₃N diffraction peak, and the shift to the right of the α -Fe diffraction peak.

Secondly, there are significant differences in the aging behaviors of nitrided W18Cr4V steel between sodium and argon. In a sodium environment at 540 °C, numerous cracks form within the nitrided layer. The diffusion of nitrogen and other alloy elements into the sodium is accelerated in the nitrided layer. However, in an argon environment, cracks do not form in the nitrided layer, and there is no accelerated diffusion of nitrogen atoms into the argon. This difference means that the diffusion rate of nitrogen atoms from the nitrided layer is significantly higher in the sodium environment than in the argon environment. Therefore, in a high-temperature-sodium environment, the microhardness of the nitrided layer of W18Cr4V steel would decrease much more significantly than in argon.

Thirdly, accelerated aging tests conducted in a sodium environment at a temperature of 700 °C revealed the long-term service behaviors of nitrided W18Cr4V steel and non-nitrided W18Cr4V steel. With the loss of a large number of nitrogen atoms, the difference in hardness between nitrided W18Cr4V steel and non-nitrided W18Cr4V steel become smaller after long-term service, and in some cases, the hardness of nitrided W18Cr4V steel is even lower than that of non-nitrided W18Cr4V steel.

Author Contributions: Conceptualization, X.F. and W.Z.; methodology, X.F., W.Z. and N.L.; validation, L.T. and Z.R.; formal analysis, B.Q. and Z.R.; investigation, N.L.; resources, L.T. and B.Q.; data curation, X.F.; writing—original draft preparation, X.F.; writing—review and editing, B.L. and S.L.; visualization, X.F.; supervision, B.L.; project administration, B.L. and X.F.; funding acquisition, S.L. and X.F. All authors have read and agreed to the published version of the manuscript.

Funding: This study was funded by the China Atomic Energy Authority Innovation Center of Nuclear Materials Cooperative Project (Grant No. ICMW-2022-Y2).

Data Availability Statement: Data are contained within the article.

Conflicts of Interest: The authors declare no conflicts of interest.

References

1. Abram, T.; Ion, S. Generation-IV nuclear power: A review of the state of the science. *Energy Policy* **2008**, *36*, 4323–4330. [[CrossRef](#)]
2. Aoto, K.; Dufour, P. A summary of sodium-cooled fast reactor development. *Prog. Nucl. Energy* **2014**, *77*, 247–265. [[CrossRef](#)]
3. Xu, M.; Yang, H.Y. Safety properties of sodium-cooled fast reactors. *Physics* **2016**, *45*, 561–568.
4. Ichimiya, M. The status of generation IV Sodium-Cooled Fast Reactor technology development and its future Project. *Energy Procedia* **2011**, *7*, 79–87. [[CrossRef](#)]
5. Rodina, E.A.; Egorov, A.V.; Rachkov, V.I.; Khomiakov, I.S. Modeling and comparative analysis of changeover of homogeneous and heterogeneous core of BN-1200 reactor to equilibrium mode. *Nucl. Eng. Des.* **2022**, *386*, 111549. [[CrossRef](#)]
6. Takano, K.; Ohki, S.; Ozawa, T.; Yamano, H.; Kubo, S.; Ogura, M.; Yamada, Y.; Koyama, K.; Kurita, K.; Costes, L.; et al. Core and safety design for France–Japan common concept on sodium-cooled fast reactor. *EPJ Nucl. Sci. Technol.* **2022**, *8*, 35. [[CrossRef](#)]
7. Lee, S.; Jeong, Y.H. Inherent safety enhancement by design optimization of a floating absorber for safety at transient (FAST) in an advanced burner reactor. *Ann. Nucl. Energy* **2022**, *172*, 109026. [[CrossRef](#)]
8. Tashlykov, O.L.; Dolgii, Y.F.; Sesekin, A.N. Optimization of refueling times in fast neutron reactors. In *IOP Conference Series: Materials Science and Engineering*; IOP Publishing: Bristol, UK, 2021. [[CrossRef](#)]
9. Dushev, S.A.; Timofeev, A.V.; Lyubimov, M.A.; Belinskii, D.L. Refueling system for fast reactors: Creation and development. *At. Energy* **2020**, *129*, 87–92. [[CrossRef](#)]
10. Kim, K.S.; Kim, J.B.; Park, C.G. Conceptual designs and characteristic of the fuel handling and transfer system for 150 MWe PGSFR and 1400 MWe SFR burner reactor. *Nucl. Eng. Technol.* **2022**, *54*, 4125–4133. [[CrossRef](#)]
11. Yan, H.; Yang, H.Y.; Yang, C. Refueling system reliability research about sodium-cooled fast reactor. *At. Energy Sci. Technol.* **2021**, *55*, 672–677.
12. Wang, M.Z.; Dong, S.G.; Song, Q.; Yang, K.L.; Gu, J.P.; Yan, H.; Wang, C.L.; Yu, T.J.; Jin, F.L.; Ma, H.S.; et al. The verifying test of refueling system of the China Experimental Fast Reactor. *Chin. J. Nucl. Sci. Eng.* **2008**, *28*, 210–217.

13. Natesan, K. Influence of nonmetallic elements on the compatibility of structural materials with liquid alkali metals. *J. Nucl. Mater.* **1983**, *115*, 251–262. [[CrossRef](#)]
14. Dai, Y.N.; Zheng, X.T.; Ding, P.S. Review on sodium corrosion evolution of nuclear-grade 316 stainless steel for sodium-cooled fast reactor applications. *Nucl. Eng. Technol.* **2021**, *53*, 3474–3490. [[CrossRef](#)]
15. Fidler, R.S.; Collins, M.J. A review of corrosion and mass transport in liquid sodium and the effects on the mechanical properties. *At. Energy Rev.* **1965**, *12*, 3–50.
16. Sivaibharasi, N.; Krishna, N.G.; Shankar, A.R.; Krishnakumar, S.; Chandramouli, S.; Karki, V.; Kannan, S.; Philip, J. Influence of long term sodium exposure on the corrosion and tensile properties of AISI type 316LN stainless steel and modified 9Cr-1Mo steel. *J. Nucl. Mater.* **2022**, *567*, 153830. [[CrossRef](#)]
17. Emami, M.; Ghasemi, H.M.; Rassizadehghan, J. High temperature tribological behaviour of 31CrMoV9 gas nitrided steel. *Surf. Eng.* **2010**, *26*, 168–172. [[CrossRef](#)]
18. Gerasimov, S.A.; Zhikharev, A.V.; Berezina, E.V.; Zubarev, G.I.; Pryanichnikov, V.A. New ideas on the mechanism of structure formation in nitrided steels. *Met. Sci. Heat Treat.* **2004**, *46*, 13–17. [[CrossRef](#)]
19. Sun, D.S.; Li, F.Z.; Dai, J.Y.; Li, D.X. Crystal defects and interface structure of ion-nitrided layers. *Acta Metall. Sin.* **1993**, *29*, 203–207.
20. Xi, Y.T.; Liu, D.X.; Han, D.; Han, Z.F. Improvement of mechanical properties of martensitic stainless steel by plasma nitriding at low temperature. *Acta Metall. Sin. (Engl. Lett.)* **2008**, *21*, 21–29. [[CrossRef](#)]
21. Karami, M.B.; Gerçekcioglu, E. Wear behaviour of plasma nitrided steels at ambient and elevated temperatures. *Wear* **2000**, *243*, 76–84. [[CrossRef](#)]
22. Chen, X.D.; Feng, S.; Wang, L.W.; Tang, R.; Zhang, F.; Ming, S.L.; Cai, Z.B. Effect of QPQ on the fretting wear behavior of TP316H steel at varying temperatures in liquid sodium. *J. Nucl. Mater.* **2022**, *562*, 153583. [[CrossRef](#)]
23. Chen, X.D.; Feng, S.; Wang, L.W.; Zhang, F.; Shi, Z.Y.; Ming, S.L.; Li, Y.; Liu, B.; Cai, Z.B. Effect of salt bath temperature on microstructure and fretting wear of nitrided 2.25Cr-1Mo steel in liquid sodium. *Appl. Surf. Sci.* **2022**, *606*, 154988. [[CrossRef](#)]
24. Johnson, R.N.; Schrock, S.L.; Whitlow, G.A. Wear resistant coatings for reactor components in liquid sodium environments. *J. Vac. Sci. Technol.* **1974**, *11*, 759–764. [[CrossRef](#)]
25. Johnson, R.N. Coatings for fast breeder reactor components. *Thin Solid Film* **1984**, *118*, 31–47. [[CrossRef](#)]
26. Hemant, K.; Ramakrishnan, V.; Albert, S.K.; Bhaduri, A.K.; Ray, K.K. Friction and wear behaviour of Ni-Cr-B hardface coating on 316LN stainless steel in liquid sodium at elevated temperature. *J. Nucl. Mater.* **2017**, *495*, 431–437.
27. Zhou, S.L.; Zhang, Z.; Zhang, J.; Wang, J.M.; Zhang, Z.G. Microstructure and wear resistance of TiAlZrCr/(Ti,Al,Zr,Cr)N gradient films deposited by multi-arc ion plating. *Acta Metall. Sin.* **2016**, *52*, 747–754.
28. Junho, C.; Koji, S.; Takahisa, K.; Masahiro, K.; Wonsik, L. Nitriding of high speed steel by bipolar PBII for improvement in adhesion strength of DLC films. *Nucl. Instrum. Methods Phys. Res. B* **2012**, *272*, 357–360.
29. He, J.L.; Chen, K.C.; Davison, A. Improvements in the understanding and application of duplex coating systems using arc plasma technology. *Surf. Coat. Technol.* **2005**, *200*, 1464–1471. [[CrossRef](#)]
30. Sharma, A.; Swami, K.C. A Study of Plasma Nitriding Process on the AISI 4140 Steel. *J. Mater. Sci. Surf. Eng.* **2014**, *1*, 81–83.
31. Wang, D.; Zhou, Y.W.; Zhang, K.C.; Su, Z.W.; Du, F.; Wu, J.S.; Guo, C. Study on diffusion behavior of nitrogen in typical steel by ionic nitriding. *Mater. Rep.* **2022**, *36*, 1–6.
32. Larson, F.R.; Miller, J. A Time-Temperature Relationship for Rupture and Creep Stresses. *Trans. Am. Soc. Mech. Eng.* **1952**, *74*, 765–771. [[CrossRef](#)]

Disclaimer/Publisher’s Note: The statements, opinions and data contained in all publications are solely those of the individual author(s) and contributor(s) and not of MDPI and/or the editor(s). MDPI and/or the editor(s) disclaim responsibility for any injury to people or property resulting from any ideas, methods, instructions or products referred to in the content.